Medical Engineering and Physics 124 (2024) 104099

Contents lists available at ScienceDirect

Medical Engineering and Physics

journal homepage: www.elsevier.com/locate/medengphy

On the relation between tidal and forced spirometry

Rutger H.J. Hebbink [a,*], Judith Elshof [b,c], Peter J. Wijkstra [b,c], Marieke L. Duiverman [b,c], Rob Hagmeijer [a]

[a] Engineering Fluid Dynamics, University of Twente, PO Box 217, 7500 AE Enschede, the Netherlands
[b] Department of Pulmonary Diseases/Home Mechanical Ventilation, University of Groningen, University Medical Center, Groningen, the Netherlands
[c] Groningen Research Institute for Asthma and COPD, University of Groningen, the Netherlands

ARTICLE INFO

Keywords:
Flow-volume curves
Obstructive lung diseases
Nasal cannula
Tidal spirometry
Respiratory monitoring

ABSTRACT

Spirometry is a lung function test involving deep inhalation and forceful deep exhalation. It is widely used to obtain objective information about airflow limitation and to diagnose lung diseases. In contrast, tidal spirometry is based on normal breathing and therefore much more convenient, but it is hardly used in medical care and its relation with conventional (forced) spirometry is largely unknown. Therefore, the objective of this work is to reveal the relation between tidal and forced spirometry. Employing the strong correspondence between the forced flow-volume curves and the Tiffeneau-Pinelli (TP) index, we present a method to obtain (a) the expected tidal flow-volume curve for a given TP-index, and (b) the expected TP-index for a given tidal curve. For patients with similar values of the TP-index, the tidal curves show a larger spread than the forced curves, but their average shape varies in a characteristic way with varying index. Therefore, just as with forced curves, the TP-index provides a useful objective ranking of the average of tidal curves: upon decreasing TP-index the expiratory flow rate changes in that its peak shifts towards smaller expiratory volumes, and its post-peak part becomes dented.

1. Introduction

Spirometry is the gold standard for measuring airflow limitation [1]. During a spirometry test, a patient inhales maximally and exhales both forcefully and maximally, while connected to the mouth piece of a spirometer and wearing a nose clip. Flow rate and volume are recorded, and the manoeuvre is repeated until at least three acceptable and repeatable measurements of the FEV_1 (volume expired during the first second of the forced expiration manoeuvre) and the FVC (forced vital capacity) are obtained, with a maximum of eight measurements to avoid the influence of fatigue [2,3].

These tests are used to diagnose and monitor pulmonary diseases [4]. Airway obstructions can be detected by looking at the shape of the expiratory part of the flow-volume curve [2–4], which strongly correlates with the value of the Tiffeneau-Pinelli (TP) index [5–9] defined as the ratio of FEV_1 and FVC:

$$I \equiv \mathrm{FEV}_1/\mathrm{FVC}. \tag{1}$$

To some extend spirometry can also be performed at home, but FEV_1 measured at home is often lower than measured in clinic [10,11] where the test is supervised and guided by a medical assistant. One of the underlying reasons is that the required effort for a successful spirometry test is difficult to overcome, not only for young children and elderly people [12,13], but also for all other ages as was shown by an international survey where 89% of the respondents was between 18 and 70 years [14].

An interesting technique complementary to forced (conventional) spirometry that can be used at home is tidal spirometry: it is based on normal breathing and doesn't require a forced manoeuvre. Tidal breathing patterns are known to also be influenced by obstructive lung diseases, as was shown both for adults [13,15–18] and for infants [19–21].

Convenient monitoring of tidal breathing recently became feasible by the development of a novel and easy-to-use method to obtain scaled tidal flow-volume curves from pressure measurements via a nasal cannula [25]. The method has been validated *in-vitro* by applying the method to 3D printed upper airways with an imposed flow-volume curve as input, and the pressure-based reconstructed flow-volume curve as output. Comparison of the two families of flow-volume curves revealed a high level of accuracy. It is noted that *in-vivo* validation of the method in patients is quite difficult since the nasal cannula measure-

* Corresponding author.
E-mail address: r.h.j.hebbink@utwente.nl (R.H.J. Hebbink).

https://doi.org/10.1016/j.medengphy.2024.104099
Received 8 August 2023; Received in revised form 12 December 2023; Accepted 1 January 2024
Available online 8 January 2024

ment implies an open system which means that the expired volume can not be measured directly. Furthermore, from a fluid mechanical point of view the differences between the *in-vitro* and *in-vivo* configurations are mainly due to the walls of the airways being rigid instead of elastic, which leads to small deviations of a few percent [22].

Compared to conventional spirometry, tidal spirometry is fairly unknown, and while forced spirometric curves are characterized by the TP-index, tidal spirometric curves do not yet have such a characterization. This raises the following question: what is the relation between the shape of a tidal curve on the one hand, and the shape of the corresponding forced curve and its TP-index on the other? Employing the strong correspondence between the forced flow-volume curves and the TP-index, the current investigation addresses the above-stated question in terms of the following two objectives:

1. given the value of the TP-index, determine the expected shape of the tidal flow-volume curve, and
2. given the shape of a tidal flow-volume curve, determine the expected value of the TP-index.

To achieve these objectives, tidal and forced curves have been measured in a group of 58 patients, and a method to accurately parametrize and compare the resulting flow volume curves has been developed, based on a projection of the expiratory part of flow-volume curves onto a series of Legendre polynomials. All of this is described in Section 2, the results are presented in Section 3, discussed in Section 4, and conclusions are drawn in Section 5.

2. Methods

The present study is observational. Measurements were conducted in the University Medical Center Groningen (UMCG), and approval to conduct the study was obtained from the local review committee of the UMCG. Written informed consent was obtained from all participating patients, and all experiments were performed in accordance with the relevant guidelines and regulations.

2.1. Patients

Measurements were obtained in two groups of subjects, the characteristics of all participants (both groups combined) are given in Table 1.

The first group of subjects consisted of 50 adults, containing both healthy subjects and patients with a variety of lung diseases. Subjects were asked to volunteer in this study when coming to hospital for standard care forced spirometry anyway, and informed consent was asked. Patients in this group were measured between December 2021 and April 2022.

The second group consisted of 8 COPD patients with an exacerbation requiring hospitalization. As part of a clinical trial, these patients received Nasal High-Flow Therapy (Airvo 2, Fisher & Paykel Healthcare Ltd., New Zealand) as treatment. Patients were measured at hospitalization, at discharge, two weeks after discharge and three months after discharge. Measurements were taken between December 2018 and July 2020.

2.2. Measurements

Two different types of measurements were performed in this study:

1. Tidal: a nasal pressure recording through a nasal cannula during two minutes of tidal breathing, mouth closed.
2. Forced: a conventional spirometry test, nose closed (clip).

Tidal curves were obtained by measuring pressure at the nose and was recorded with a pressure sensor connected to a nasal cannula. In the first patient group, the pressure sensor (SDP810-500Pa, Sensirion, Switzerland) was connected to the end of a standard oxygen nasal cannula. In the second patient group, pressure was measured (PXM409-070HCGUSBH, Omega Engineering Inc., USA) between the heated tube and the Nasal High-Flow cannula (OPT944, Fisher & Paykel Healthcare Ltd., New Zealand) while the device was turned off, such that breathing patterns were not influenced by the therapy.

Table 1
Participant characteristics. Age, length and weight are specified as mean ± standard deviation.

Male/Female subjects	17/41
Age [years]	54.0 ± 16.9
Height [cm]	169 ± 8.1
Weight [kg]	71.5 ± 17.5
Underlying disease:	
– Asthma	2
– Asthma-COPD overlap syndrome	2
– COPD	13
– COPD exacerbation	8
– Cystic fibrosis	3
– Post lung transplantation	11
– Neuromuscular diseases	3
– No pulmonary disease	16

Forced spirometry was performed according to the ERS guidelines [3]. Therefore, at least three acceptable flow-volume curves were obtained. The flow-volume curve with the best expiration was used for analysis in this study. The parameters FEV_1 and FVC were taken as the maximum values among the acceptable curves (which may come from different curves) [4]. Because of the required effort, forced spirometry measurements in the exacerbation patient group could not be obtained at hospitalization, but only at and after discharge.

2.3. Data processing

The pressure signal of the tidal measurements was smoothed by applying a 9-point moving-mean filter, and the scaled flow rate and volume, $\widetilde{Q}(t)$ and $\widetilde{V}(t)$ respectively, were reconstructed following the method presented in [22]. Individual breathing cycles were obtained by identifying the minima in $\widetilde{Q}$, such that all cycles start and end at peak inhalation. It is noted that both $\widetilde{Q}$ and $\widetilde{V}$ are dimensionless, and that $\widetilde{V}$ has been scaled and centered such that its minimum and maximum value are -1 and 1 respectively. The focus in this work is on the expiratory part of flow-volume curves, since this is the most important part in monitoring obstructive pulmonary diseases [23–26].

For every subject a single (expiratory) tidal flow-volume curve was obtained by averaging the individual breathing cycles. This is illustrated in Supplementary Fig. S1 (online, MMC 1) for two patients, one with relatively low and one with relatively high variation between the individual breathing cycles. It is observed that the average curves indeed have very similar shapes when compared to the underlying individual flow-volume curves, and therefore are adequate representatives. The mathematical approach to calculate the subject's flow-volume curve from the individual breathing cycles is explained later in Section 2.6.

It is noted that individual breathing cycles were projected on a series of 15 to 20 Legendre polynomials, and the resulting curve was obtained by averaging typically 10 to 20 of these curves. Therefore there seems no concern of overfitting.

2.4. Illustration of the main idea: expected values

To explain the main idea of this work, it is temporarily assumed that the shape of a tidal flow-volume curve can be characterized by a single shape parameter, say α. One could for example think of the average curvature of the curve. The question of finding the relation between the shape of the tidal flow-volume curve and the TP-index

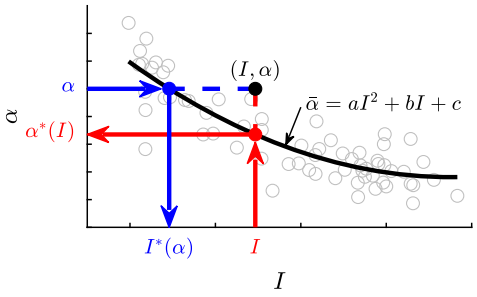

Fig. 1. Illustration of the main idea. Each gray circle denotes the measured values of I (TP-index) and α (shape parameter of the tidal flow-volume curve) of a subject. The black line indicates the curve fit given by Eq. (2). For a selected subject, marked by the black circle, the expected value of the shape parameter, α^*, is determined by finding the intersection of the *vertical* line through the point (I,α) and the curve fit (red arrows). Similarly, the expected value of the TP-index, I^*, is determined by finding the intersection of the *horizontal* line through the point (I,α) and the curve fit (blue arrows).

I then transforms into the equivalent question of finding the relation between α and I.

The scatter plot in Fig. 1 shows typical measured values of α and I, where each pair of these values is indicated by a gray circle. Based on these data, a second-order curve-fit through the data points is computed,

$$\bar{\alpha}(I) = aI^2 + bI + c, \tag{2}$$

where the coefficients a, b, and c are determined by least-squares minimization. The function $\bar{\alpha}(I)$ represents a single-parameter family of *expected* shapes, and therefore a single-parameter family of *expected* flow-volume curves as a function of known TP-index.

Now consider a particular combination (α, I) of the shape of the flow-volume curve and the TP-index of a subject, indicated by the black circle in Fig. 1. If only the value of the TP-index is known, the *expected* shape, or equivalently, the expected value of α, denoted by α^*, can be determined by evaluating the curve fit of Eq. (2) at the measured value of I. Graphically, one is looking for the intersection between the vertical line through (α, I) and the curve fit. On average, the value of the TP-index given by I will correspond to a shape given by α^*.

Similarly, if only the shape is known, the *expected* value of the TP-index, denoted by I^*, can be determined by looking for the intersection between the horizontal line through (α, I) and the curve fit, and by taking I^* equal to the value of I belonging to the intersection point. This provides a classification of the shape of the flow-volume curves: on average, the shape given by α will correspond to a TP-index equal to I^*.

2.5. The main idea in full detail

2.5.1. Multi-parameter representation

Several attempts have been made to describe the shape of flow-volume curves, both forced and tidal, by one parameter (related to the curvature of the decreasing expiratory part of the curve) [24–26], or by a few parameters (evaluating the expiratory flow compared to the peak expiratory flow at a number of relative expired volumes) [19,27]. However, none of these methods allow for an accurate reconstruction of the flow-volume curve from the parameters only, and that is exactly what is needed in this work.

Therefore, a new multi-parameter approach is used here, based on expressing each tidal flow-volume curve in a series of N Legendre polynomials P_n (see Supplementary Methods online, MMC 2):

$$\widetilde{Q}(\widetilde{V}) \approx \sum_{n=0}^{N-1} \alpha_n P_n(\widetilde{V}). \tag{3}$$

The amplitudes α_n are the 'shape parameters' that characterize the flow-volume curve. Given a measured tidal flow-volume curve $\widetilde{Q}(\widetilde{V})$, these are conveniently computed as:

$$\alpha_n = \frac{2n+1}{2} \int_{-1}^{1} \widetilde{Q}(\widetilde{V}) P_n(\widetilde{V}) \mathrm{d}\widetilde{V}. \tag{4}$$

When the number of terms in the series in Eq. (3) is increased, the accuracy of the series representation is also increased. In fact, any required accuracy can be reached. As shown in the Supplementary Methods, $N = 15$ leads to a sufficiently accurate description of tidal flow-volume curves, and $N = 20$ leads to a sufficiently accurate description of forced flow-volume curves.

2.5.2. Multiple curve-fits

For every shape parameter α_n separately, with $n = 0, 1, 2, ..., N-1$, a scatter plot such as Fig. 1 is made with α_n on the vertical axis and I on the horizontal axis. This results in a number of N scatter plots. All of the N shape parameters are then curve-fitted separately by second order polynomials:

$$\bar{\alpha}_n(I) = a_n I^2 + b_n I + c_n, \quad n = 0, 1, ..., N-1. \tag{5}$$

These curve fits form the basis for the approach outlined in the next three paragraphs.

2.5.3. Expected shape for a given TP-index

If only the value of the TP-index is known, the *expected* shape of the flow-volume curve, or equivalently, the expected values of α_n, denoted by α_n^*, can be determined by evaluating the curve fits of Eq. (5) at the measured value of I. The expected tidal flow-volume curve is now simply obtained by substituting the expected shape parameters in a truncated series of Legendre polynomials (see Eq. (3)):

$$\alpha_n^* = \bar{\alpha}_n(I), \quad \widetilde{Q}^*(\widetilde{V}, I) = \sum_{n=0}^{N-1} \alpha_n^* P_n(\widetilde{V}). \tag{6}$$

2.5.4. Expected TP-index for a given shape

If only the shape of the tidal flow-volume curve is known in terms of the shape parameters α_n, $n = 0, 1, 2, ..., N-1$, it is not straightforward to find the expected value of the TP-index, denoted by I^*. The reason is that, ideally, all of the N equations $\bar{\alpha}_n(I^*) = \alpha_n$ have to be satisfied by a single value of I^*, which in general is not possible. Therefore, the expected TP-index I^* is defined as the value of I that optimally satisfies the N equations in the least squares sense, i.e., that minimizes the error

$$\epsilon^2(I^*) \equiv \frac{1}{2} \sum_{n=0}^{N-1} \frac{2}{2n+1} (\bar{\alpha}_n(I^*) - \alpha_n)^2. \tag{7}$$

2.5.5. Best-matching flow-volume curve

The error ϵ denotes the L_2-norm[1] of the difference between the shape of the flow-volume curve at I^* and the measured flow-volume curve (see Supplementary Methods). Therefore, the flow-volume curve at I^* is referred to as the 'best-matching flow-volume curve':

$$\widetilde{Q}^{**}(\widetilde{V}, I^*) = \sum_{n=0}^{N-1} \bar{\alpha}_n(I^*) P_n(\widetilde{V}). \tag{8}$$

In the exceptional case that ϵ is zero, the best-matching curve is exactly equal to the measured curve. Since the expression for ϵ^2 is fourth order in I^*, maximally two local minima are present. The smallest minimum value is used, but only values of I^* within the measured range of I are considered.

[1] The L_2-norm is the Root-Mean-Square (RMS) of the differences of the two sets of Legendre coefficients corresponding to the two curves that are compared.

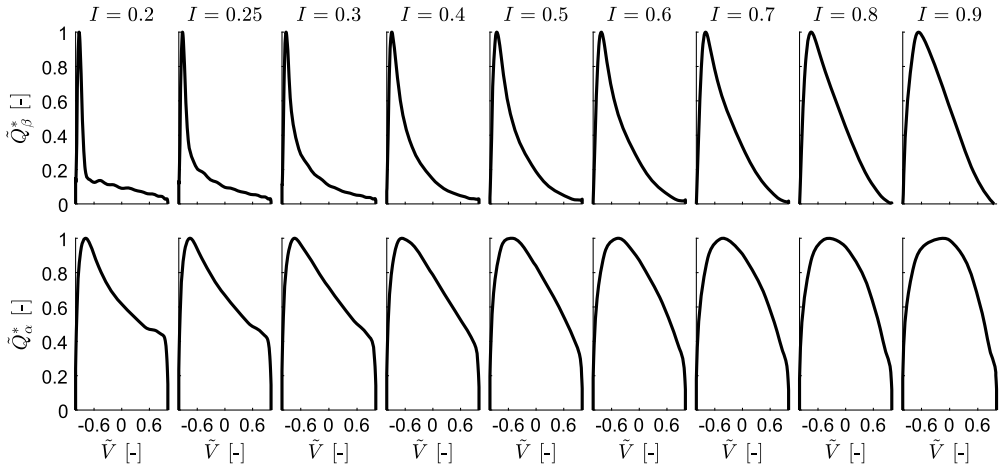

Fig. 2. Expected forced (top row) and expected tidal (bottom row) flow-volume curves for a range of values of the TP-index I (indicated above each column), as given by Eq. (6). Both families of curves show smooth and monotonic variation with decreasing TP-index: (a) the expiratory peak shifts towards smaller expiratory volumes, and (b) the post-peak part becomes dented. $\widetilde{Q}$: scaled expiratory flow rate; $\widetilde{V}$: scaled volume.

2.6. Averaging and scaling

A subject's tidal flow-volume curve is determined by averaging over the individual breathing cycles, which is conveniently achieved by averaging the shape parameters of the individual breathing cycles, see the Supplementary Methods. To facilitate a proper comparison of the tidal flow-volume curves of different subjects, the dimensionless flow rate is re-scaled to a maximum of one. This actually means that the shape parameters of a subject's flow-volume curve are all scaled by the same factor.

2.7. Terminology

The methods described above are applied to both tidal flow-volume curves and forced flow-volume curves. In the remainder of this work, the coefficients α_n refer to the shape parameters of a tidal curve, whereas the coefficients β_n refer to the shape parameters of a forced curve. Also, the *subscript* α indicates 'tidal' or 'obtained from tidal curves', such as a measured tidal flow-volume curve $\widetilde{Q}_\alpha(\widetilde{V})$, an expected tidal flow-volume curve $\widetilde{Q}^*_\alpha(\widetilde{V}, I)$, or an expected TP-index I^*_α corresponding to a tidal curve. Similarly, the *subscript* β indicates 'forced' or 'obtained from forced curves'.

3. Results

3.1. Expected shape for a given TP-index

An overview of the expected flow-volume curves $\widetilde{Q}^*(\widetilde{V}, I)$ for a range of values of the TP-index I (obtained by inserting values for I in Eq. (6)), is shown in Fig. 2 for both forced and tidal curves. In both cases, the expected curve shape varies smoothly and monotonically with varying TP-index. Although the shapes of the forced and tidal curves are different, two trends for decreasing values of I appear to be common: (a) the expiratory peak shifts towards smaller expiratory volumes, and (b) the post-peak part becomes dented. It is also observed that the transition from expiration to inhalation in the tidal curves, close to maximum expired volume, is very sudden at low values of I, but gradual at larger values.

For the expected tidal flow-volume curves depicted in Fig. 2, Fig. 3 shows the ratio of the expired volume $\Delta\widetilde{V}$ at which the peak occurs (relative to -1) divided by the total tidal volume $\widetilde{V}_T$, together with a linear curve fit. The slope of the curve fit is 0.43, which is nearly identical to the slope of 0.42 found by Morris and Lane [15] using a constant volume whole body plethysmograph and a heated pneumotachograph to measure tidal curves in 99 subjects.

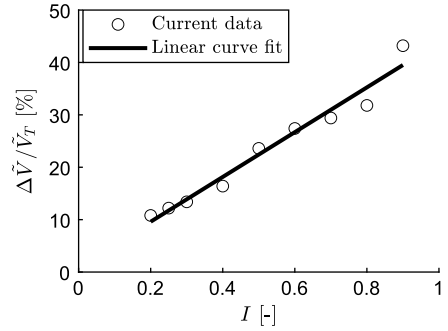

Fig. 3. Ratio of the volume at which the expiratory peak occurs, divided by the total tidal volume, for the expected tidal flow-volume curves depicted in Fig. 2. The slope of the linear curve fit is 0.43.

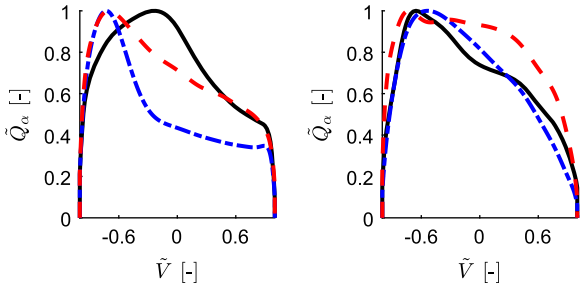

Fig. 4. Examples of measured tidal flow-volume curves. Left: three subjects with $I \approx 0.24$. Right: three subjects with $I \approx 0.80$. In both figures, the different linetypes and colors denote different subjects. $\widetilde{Q}$: scaled expiratory flow rate; $\widetilde{V}$: scaled volume.

Supplementary Figs. S2 and S3 (online, MMC 1) show the measured shape parameters α_n (tidal curves) and β_n (forced curves) versus the TP-index I, and their corresponding curve-fits $\bar{\alpha}_n(I)$ and $\bar{\beta}_n(I)$ (see Eq. (5)). The values of the coefficients of the curve-fits are given in the Supplementary Data (online, MMC 3).

When looking at similar values of the measured TP-index, a relatively large range of values for α_n is observed, indicating a large variety of tidal-curve shapes. This variety is illustrated in Fig. 4, where the tidal curves of six subjects for two values of I are presented. In contrast, the corresponding values of β_n show relatively small variation, which confirms the strong correlation between the shape of the forced flow-volume curves and the corresponding values of the TP-index.

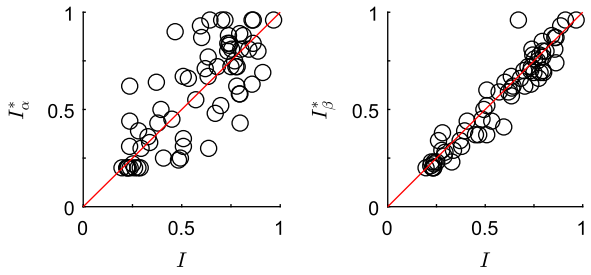

(a) Tidal curves (b) Forced curves

Fig. 5. Expected TP-index I^* against the measured TP-index I (see Eq. (7)) for tidal (a) and forced (b) curves. The lines $I^* = I$ are depicted in red: points above these lines represent curves that are more favorable ($I^* > I$), and points below these lines represent curves that are less favorable ($I^* < I$).

3.2. Expected TP-index from measured flow-volume curves

The expected TP-index I^* of tidal and forced curves is plotted against the measured TP-index I in Fig. 5a and b, respectively. The lines $I^* = I$ are depicted in red: points above these lines represent more favorable flow-volume curves ($I^* > I$), and points below these lines represent less favorable curves ($I^* < I$).

For the tidal curves, considerable variation of I^*_α with respect to the red line is observed, which confirms the relatively large variety of tidal curves at similar values of the TP-index. Linear regression leads to a statistically significant model ($R^2 = 0.59$, $F = 93.9$, $p < 0.001$):

$$I^*_\alpha \approx 0.0781 + 0.8857\, I. \tag{9}$$

The small value of R^2 confirms the moderate correlation between the shape of the tidal curves and the TP-index.

For the forced curves, limited variation of I^*_β with respect to the red line is observed, which confirms the relatively small variety of forced curves at similar values of the TP-index. One data point clearly appears as an outlier compared to the other measurements. The outlier corresponds to an irregularly shaped curve where the increase towards peak expiration is not smooth. Linear regression also in this case leads to a statistically significant model ($R^2 = 0.92$, $F = 700$, $p < 0.001$):

$$I^*_\beta \approx -0.0149 + 0.9960\, I. \tag{10}$$

The value of R^2 being very close to 1 confirms the expected strong correlation between the shape of the forced curves and the TP-index. The slope of the regression line being very close to 1, and the constant being very close to 0, indicates that the expected index I^*_β is almost equal to the measured index I.

To visualize how the measured tidal curves and the relevant reference curves relate to each other, the measured tidal curve $\widetilde{Q}_\alpha(\widetilde{V})$, the expected tidal curve $\widetilde{Q}^*_\alpha(\widetilde{V}, I)$, and the best-matching tidal curve are shown for a selection of three subjects in Fig. 6a. In all three cases, the measured curve and the expected curve are quite different, whereas the measured curve and the best-matching curve are much more similar. This observation is confirmed by the small values of ϵ. The difference between the expected curve and the best-matching curve exemplifies the earlier observed difference between forced and tidal spirometry (see Fig. 5a).

For the same three subjects, the corresponding forced curves are shown in Fig. 6b. In all three cases, both the measured curve, the expected curve, and the best-matching curve are quite similar, which reflects the strong correlation between the shape of the forced curve and the value of I.

The complete set of figures similar to those presented in Fig. 6 for all subjects can be found as Supplementary Figs. S4 and S5 (online, MMC 1). The distribution of the relative differences ϵ between the measured curves and their corresponding calculated best-matching curves is shown in the histograms presented in Fig. 7. In line with earlier observations, the width of the tidal data in Fig. 7a is larger than the width of the forced data in Fig. 7b. This is caused by the larger variation of tidal curves compared to forced curves at given values of the TP-index. As a result, forced curves are better represented by best-matching curves compared to tidal curves. Finally, it is noted that the outlier in the forced data is also clearly visible at $\epsilon = 0.32$.

4. Discussion

Similar to how the index I represents a classification of the forced flow-volume curve of a patient, the expected index I^*_α may potentially be used to classify the tidal flow-volume curve of a patient. While a decreasing TP-index is known to reflect airway obstruction or loss of elastic recoil, or a combination of both, the pathophysiologic phenomena reflected in tidal breathing are unclear at this point. Future studies may therefore aim at relating an index of tidal breathing (for example the expected index I^*_α) to various pathophysiologic phenomena, thereby gaining better understanding of the (potential) clinical significance of tidal breathing.

Clearly, the (sometimes) considerable differences between the measured TP-index I and the expected TP-index I^*_α indicate that tidal breathing is clinically insignificant as an *alternative* to the TP-index. Since pulmonary obstructions are diagnosed based on this index [5–9], this also means that tidal curves are not useful to *detect* obstructions. However, the *severity* of obstructions is assessed by measuring FEV_1 [1]. While the TP-index is nearly insensitive to bronchodilator administration, the FEV_1 may improve [28]. Moreover, (forced) spirometric indices are known to correlate poorly with respiratory symptoms, dyspnoea, exacerbations, hospitalization, exercise limitation and quality of life, and therefore do not capture the complete clinical picture [29]. Whether tidal spirometry can contribute to this should be investigated.

The present study confirms that, as expected, the TP-index I correlates strongly with the shape of the forced flow-volume curve. Although this finding is not new [30,31], the correlation found in this study is stronger, presumably because the entire shape of the forced flow-volume curve has been used rather than specific parameters or characteristics of it. A potentially interesting application of this strong correlation is to use the forced expected curves $\widetilde{Q}^*_\beta(\widetilde{V}, I)$ to objectively accept or reject forced flow-volume curves measured by conventional spirometry: if the measured curve cannot be matched to one of the expected curves within a certain tolerance it could be rejected.

A few limitations in this study are observed. First of all, the number of subjects tested is relatively small (58). Upon using a larger data set, the distribution of the shape parameters at the same value of the TP-index will be more detailed. This may also justify the use of higher order fits through the shape parameters, which would amplify the variation in characteristic curves. Furthermore, the expected shape at low and high values of I could be investigated if subjects with extreme values of the TP-index were included, which would increase the validity range of I^*.

Secondly, the patients with COPD exacerbations were not measured at all points in time foreseen which somewhat obstructs the analysis.

Thirdly and finally, the order of tidal measurements and forced measurements was not standardized. Tidal breathing measurements may be slightly different when performed after a conventional spirometry test due to fatigue from the forced manoeuvre. However, in the cases that tidal measurements were performed after the spirometry test, there was always some time between the measurements which exceeded the usual time between two forced manoeuvres.

5. Conclusions

- The *expected* shape of tidal flow-volume curves, obtained via nasal pressure measurements, varies smoothly with varying TP-index, despite the large variation in the shape of tidal curves of subjects with similar values of the TP-index.

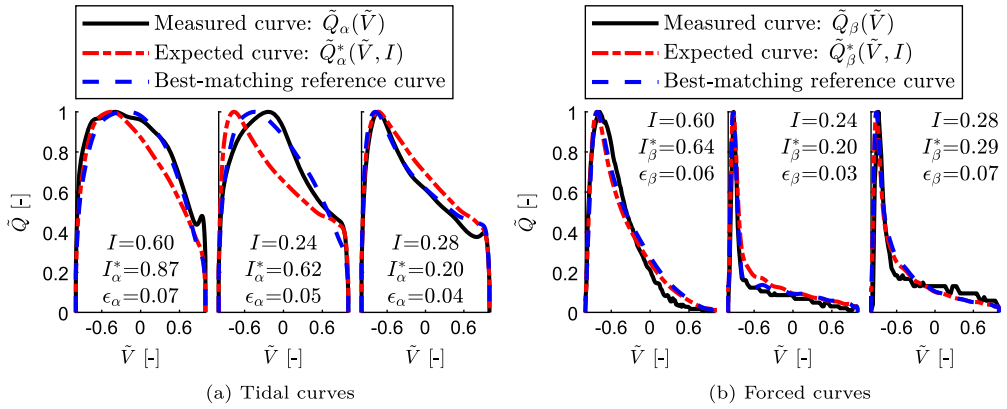

Fig. 6. Examples for three subjects (each in a different figure panel) of tidal (a) and forced (b) measured flow-volume curves (black solid lines), expected flow-volume curves (red dashed-dotted line, see Eq. (6)), and best-matching flow-volume curves (blue dashed line, see Eq. (8)). Also indicated are the values of ϵ which is defined in Eq. (7). $\tilde{Q}$: scaled expiratory flow rate; $\tilde{V}$: scaled volume.

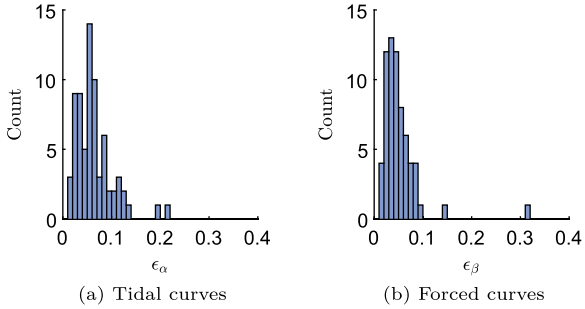

Fig. 7. L_2-norm ϵ of the difference between the best matching curve (see Eq. (7)) and the measured flow-volume curve for tidal curves (a) and forced curves (b). It is noted that $\epsilon = 0$ implies that the best matching curve is exactly equal to the measured curve.

- In tidal flow-volume curves, upon decreasing index, (a) the expiratory peak shifts towards smaller expiratory volumes, and (b) the post-peak part becomes dented.
- Tidal flow-volume curves can be classified by the *expected* TP-index, which suggests a coupling between the pulmonary-health status of a patient and its tidal respiration pattern.

CRediT authorship contribution statement

RHJH: Conceptualization, Methodology, Software, Validation, Formal analysis, Investigation, Data curation, Writing - Original draft, Writing - Review & Editing, Visualization. **JE:** Measurements, Writing - Review & Editing. **MLD:** Writing - Review & Editing, Supervision, Project administration, Funding acquisition. **PJW:** Writing - Review & Editing, Supervision. **RH:** Conceptualization, Methodology, Investigation, Writing - Original draft, Writing -Review & Editing, Supervision, Project administration, Funding acquisition.

Funding

This research is financially supported by Longfonds, Fisher & Paykel Healthcare Ltd. and Vivisol Nederland BV, under Longfonds project number 10.1.17.184. The sponsors were not involved in the study design, the collection, analysis and interpretation of data, or the writing or submission of the article.

Ethical approval

Approval to conduct the study was obtained from the local review committee of the University Medical Center Groningen and written informed consent was obtained.

Declaration of competing interest

The authors have no real or perceived conflicts of interest to declare.

Acknowledgements

The authors would like to acknowledge M. Farenhorst of the University Medical Center Groningen for his contribution in the measurement of the subjects. Furthermore they would like to express their gratitude to dr. D.S. Van Putten for reviewing the manuscript and for giving his valuable comments.

Appendix A. Supplementary material

Supplementary material related to this article can be found online at https://doi.org/10.1016/j.medengphy.2024.104099.

References

[1] Global Initiative for Chronic Obstructive Lung Disease, Inc. Global strategy for the diagnosis, management, and prevention of chronic obstructive pulmonary disease (2022 report). Tech. Rep. Global Initiative for Chronic Obstructive Lung Disease, Inc.; 2021.
[2] Richards JA. Office spirometry—indications and limitations. South Afr Fam Prac 2006;48(2):48–51. https://doi.org/10.1080/20786204.2006.10873340.
[3] Graham BL, Steenbruggen I, Miller MR, Barjaktarevic IZ, Cooper BG, Hall GL, et al. Standardization of spirometry 2019 update. An official American thoracic society and European respiratory society technical statement. Am J Respir Crit Care Med 2019;200(8):e70–88. https://doi.org/10.1164/rccm.201908-1590ST.
[4] Miller MR, Hankinson J, Brusasco V, Burgos F, Casaburi R, Coates A, et al. Standardisation of spirometry. Eur Respir J 2005;26(2):319–38. https://doi.org/10.1183/09031936.05.00034805.
[5] Pellegrino R, Viegi G, Brusasco V, Crapo RO, Burgos F, Casaburi R, et al. Interpretative strategies for lung function tests. Eur Respir J 2005;26(5):948–68. https://doi.org/10.1183/09031936.05.00035205.
[6] Quanjer PH, Tammeling GJ, Cotes JE, Pedersen OF, Peslin R, Yernault J-C. Lung volumes and forced ventilatory flows. Eur Respir J 1993;6(Suppl 16):5–40. https://doi.org/10.1183/09041950.005s1693.
[7] Hankinson JL, Odencrantz JR, Fedan KB. Spirometric reference values from a sample of the general U.S. population. Am J Respir Crit Care Med 1999;159(1):179–87. https://doi.org/10.1164/ajrccm.159.1.9712108.
[8] Quanjer PH, Stanojevic S, Cole TJ, Baur X, Hall GL, Culver BH, et al. Multi-ethnic reference values for spirometry for the 3–95-yr age range: the global lung function 2012 equations. Eur Respir J 2012;40(6):1324–43. https://doi.org/10.1183/09031936.00080312.
[9] Global Initiative for Chronic Obstructive Lung Disease, Inc. Global strategy for the diagnosis, management, and prevention of chronic obstructive pulmonary disease (2021 report). Tech. Rep. Global Initiative for Chronic Obstructive Lung Disease, Inc.; 2020.
[10] Paynter A, Khan U, Heltshe SL, Goss CH, Lechtzin N, Hamblett NM. A comparison of clinic and home spirometry as longtudinal outcomes in cystic fibrosis. J Cyst Fibros 2022;21(1):78–83. https://doi.org/10.1016/j.jcf.2021.08.013.

[11] Rodriguez-Roisin R, Tetzlaff K, Watz H, Wouters EF, Disse B, Finnigan H, et al. Daily home-based spirometry during withdrawal of inhaled corticosteroid in severe to very severe chronic obstructive pulmonary disease. Int J Chronic Obstr Pulm Dis 2016;11(1):1973–81. https://doi.org/10.2147/COPD.S106142.

[12] Lødrup Carlsen KC. Tidal breathing at all ages. Monaldi Arch Chest Dis 2000;55(5):427–34.

[13] Nozoe M, Mase K, Murakami S, Okada M, Ogino T, Matsushita K, et al. Relationship between spontaneous expiratory flow-volume curve pattern and air-flow obstruction in elderly COPD patients. Respir Care 2013;58(10):1643–8. https://doi.org/10.4187/respcare.02296.

[14] Johnson B, Steenbruggen I, Graham BL, Coleman C. Improving spirometry testing by understanding patient preferences. ERJ Open Res (Jan. 2021;7(1). https://doi.org/10.1183/23120541.00712-2020.

[15] Morris MJ, Lane DJ. Tidal expiratory flow patterns in airflow obstruction. Thorax 1981;36(2):135–42. https://doi.org/10.1136/thx.36.2.135.

[16] Colasanti RL, Morris MJ, Madgwick RG, Sutton L, Williams EM. Analysis of tidal breathing profiles in cystic fibrosis and COPD. Chest 2004;125(3):901–8. https://doi.org/10.1378/chest.125.3.901.

[17] Morris MJ, Williams EM, Madgwick R, Banerjee R, Phillips E. Changes in lung function and tidal airflow patterns after increasing extrathoracic airway resistance. Respirology 2004;9(4):474–80. https://doi.org/10.1111/j.1440-1843.2004.00612.x.

[18] Wilkens H, Weingard B, Mauro AL, Schena E, Pedotti A, Sybrecht GW, et al. Breathing pattern and chest wall volumes during exercise in patients with cystic fibrosis, pulmonary fibrosis and COPD before and after lung transplantation. Thorax 2010;65(9):808–14. https://doi.org/10.1136/thx.2009.131409.

[19] Hevroni A, Goldman A, Blank-Brachfeld M, Ahmad WA, Ben-Dov L, Springer C. Use of tidal breathing curves for evaluating expiratory airway obstruction in infants. J Asthma 2018;55(12):1331–7. https://doi.org/10.1080/02770903.2017.1414234.

[20] Leonhardt S, Ahrens P, Kecman V. Analysis of tidal breathing flow volume loops for automated lung-function diagnosis in infants. IEEE Trans Biomed Eng 2010;57(8):1945–53. https://doi.org/10.1109/TBME.2010.2046168.

[21] Schmalisch G, Wilitzki S, Wauer R. Differences in tidal breathing between infants with chronic lung diseases and healthy controls. BMC Pediatr 2005;5(1):36. https://doi.org/10.1186/1471-2431-5-36.

[22] Hebbink RHJ, Hagmeijer R. Tidal spirometric curves obtained from a nasal cannula. Med Eng Phys 2021;97:1–9. https://doi.org/10.1016/j.medengphy.2021.09.004.

[23] O'Donnell DE, Parker CM. COPD exacerbations · 3: pathophysiology. Thorax 2006;61(4):354–61. https://doi.org/10.1136/thx.2005.041830.

[24] Zheng C-J, Adams AB, McGrail MP, Marini JJ, Greaves IA. A proposed curvilinearity index for quantifying airflow obstruction. Respir Care 2006;51(1):40–5.

[25] Nève V, Matran R, Baquet G, Methlin C-M, Delille C, Boulenguez C, et al. Quantification of shape of flow-volume loop of healthy preschool children and preschool children with wheezing disorders. Pediatr Pulmonol 2012;47(9):884–94. https://doi.org/10.1002/ppul.22518.

[26] Dominelli PB, Foster GE, Guenette JA, Haverkamp HC, Eves ND, Dominelli GS, et al. Quantifying the shape of the maximal expiratory flow–volume curve in mild COPD. Respir Physiol Neurobiol 2015;219:30–5. https://doi.org/10.1016/j.resp.2015.08.002.

[27] Gólczewski T, Lubiński W. Spirometry: quantification of the shape of the maximal expiratory flow-volume curve. Biocybern Biomed Eng 2008;28(3):17–25.

[28] Dellacà RL, Pompilio PP, Walker PP, Duffy N, Pedotti A, Calverley PMA. Effect of bronchodilation on expiratory flow limitation and resting lung mechanics in COPD. Eur Respir J 2009;33(6):1329–37. https://doi.org/10.1183/09031936.00139608.

[29] Quanjer PH, Pretto JJ, Brazzale DJ, Boros PW. Grading the severity of airways obstruction: new wine in new bottles. Eur Respir J 2014;43(2):505–12. https://doi.org/10.1183/09031936.00086313.

[30] Bhatt SP, Bhakta NR, Wilson CG, Cooper CB, Barjaktarevic I, Bodduluri S, et al. New spirometry indices for detecting mild airflow obstruction. Sci Rep 2018;8(1):17484. https://doi.org/10.1038/s41598-018-35930-2.

[31] Li H, Liu C, Zhang Y, Xiao W. The concave shape of the forced expiratory flow-volume curve in 3 seconds is a practical surrogate of FEV1/FVC for the diagnosis of airway limitation in inadequate spirometry. Respir Care 2017;62(3):363–9. https://doi.org/10.4187/respcare.05016.